Article

# Systematic Control of Photochemistry: The Dynamics of Photoisomerization of a Model Cyanine Dye

Patricia A. Hunt, and Michael A. Robb

*J. Am. Chem. Soc.*, **2005**, 127 (15), 5720-5726• DOI: 10.1021/ja045652s • Publication Date (Web): 26 March 2005



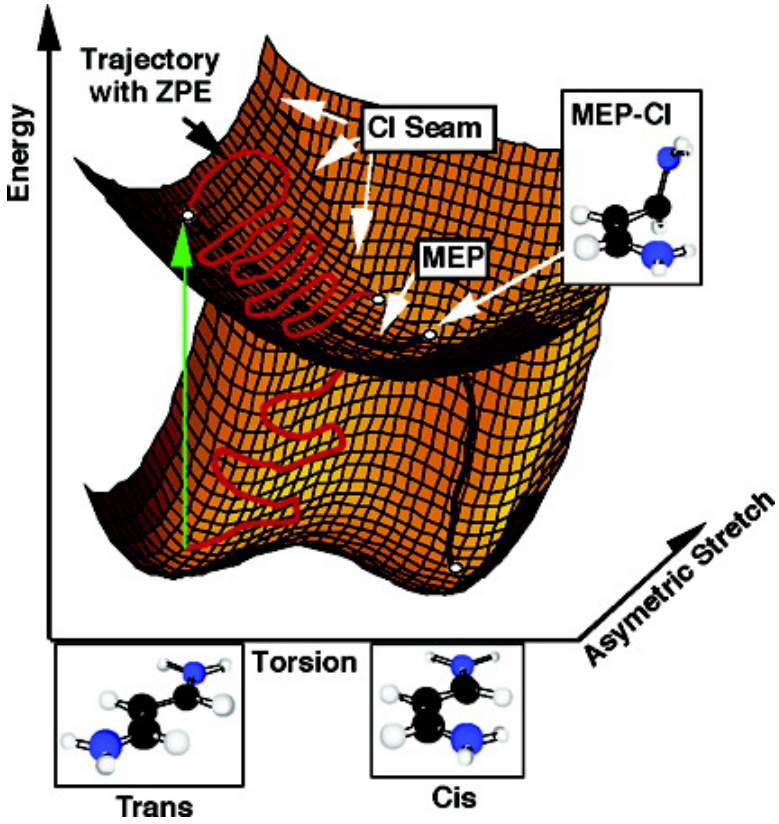


## More About This Article

Additional resources and features associated with this article are available within the HTML version:

- Supporting Information
- Links to the 9 articles that cite this article, as of the time of this article download
- Access to high resolution figures
- Links to articles and content related to this article

J|A|C|S
ARTICLES
Published on Web 03/26/2005

# Systematic Control of Photochemistry: The Dynamics of Photoisomerization of a Model Cyanine Dye

Patricia A. Hunt* and Michael A. Robb

*Contribution from the Department of Chemistry, Imperial College London, London, SW7 2AZ, United Kingdom*

Received July 20, 2004; E-mail: p.hunt@imperial.ac.uk; mike.robb@imperial.ac.uk

***Abstract:*** On-the-fly CASSCF nonadiabatic dynamics have been used to model the trans−cis isomerization of a model cyanine dye. Our results show that the photochemical generation of the trans versus cis product is dynamically controlled by the presence of an extended cis−trans conical intersection seam that persists along all torsional angles. This in turn suggests that the photochemistry could be completely controlled by controlling the distribution of momentum components in a wave packet excited by laser photolysis in a coherent control experiment.

## 1. Introduction

The possibility of using pulsed femtosecond laser light (via coherent optical control) as a new class of "chemical reagent" appears to be coming closer to reality. (See, for example, the 2004 special issue of chemical reviews devoted to femtochemistry,[1] and reviews by Rabitz and de Vivie-Riedle,[2] Brixner and Gerber,[3] and more recently by Dantus and Lozovoy.[4]) The main experimental problem is determination of the laser field. One solution, first proposed in 1992 by Judson and Rabitz,[5] has been to use a learning algorithm and feedback loop.[5−12] In these experiments ultrashort laser pulses are used to initiate and then modify a photochemical reaction. The form of the trial pulse sequence and the associated experimental "output" are then fed into an "evolutionary" optimization algorithm which determines a new pulse form. After several cycles a pulse form that generates the desired photochemical product is produced.[2,5] A key problem is the extremely large range of possible pulse forms, making optimization difficult.[1] Moreover, this approach is often implemented without any real understanding of the mechanistic processes occurring at the molecular level. The challenge, therefore, is to predict the shape of the controlling laser pulse, using *prior* knowledge of the potential energy surface.

Theoretical methods can be used to address this issue, structured laser pulses have been computationally determined using low dimensional model potentials and optimal control theory.[13−25] However, translating these designs into successful experiments has proven difficult: either the model potentials have been inadequate or the computed pulses have been too difficult to create. Wave packet propagation on low dimensional ab initio potential surfaces has recently been used to *rationalize* optimal pulse forms.[24,25] An alternative strategy may be to run theoretical dynamics on a computed potential energy surface. Knowledge of the surface topology (and reaction mechanisms) can then be used to establish either an objective for optimal control theory or limits on the (experimental) search for a pulse form. However, it is not at all obvious which type of molecular systems will be amenable to this approach. In this paper we present a theoretical study of the dynamics of a model cyanine dye. Because of the unusual potential surface topology, involving an extended low-energy conical intersection seam, we believe this type of system might be a useful prototype for design of a coherent control experiment.

When a femtosecond light pulse interacts with a polyatomic molecule it excites a coherent superposition of vibrational modes, creating a nuclear wave packet on an electronic excited-

(1) Dantus, M., Zewail, A. *Chem. Rev.* **2004**, *104*, 1717.
(2) Rabitz, H.; de Vivie-Riedle, R.; Motzkus, M.; Kompa, K. *Science* **2000**, *288*, 824.
(3) Brixner, T.; Gerber, G. *ChemPhysChem* **2003**, *4*, 418.
(4) Dantus, M.; Lozovoy, V. *Chem. Rev.* **2004**, *104*, 1813.
(5) Judson, R.; Rabitz, H. *Phys. Rev. Lett.* **1992**, *68*, 1500.
(6) Bardeen, C.; Yakovlev, V.; Wilson, K.; Carpenter, S.; Weber, P.; Warren, W. *Chem. Phys. Lett* **1997**, *280*, 151.
(7) Daniel, C.; Full, J.; González, L.; Kaposta, C.; Krenz, M.; Lupulescu, C.; Manz, J.; Minemoto, S.; Oppel, M.; Rosendo-Francisco, P.; Vajda, S.; Wöste, L. *Chem. Phys.* **2001**, *267*, 247.
(8) Assion, A.; Baumert, T.; Bergt, M.; Brixner, T.; Kiefer, B.; Seyfried, V.; Struhle, M.; Gerber, G. *Science* **1998**, *282*, 919.
(9) Levis, R.; Menkir, G.; Rabitz, H. *Science* **2001**, *292*, 709.
(10) Brixner, T.; Damrauer, N.; Niklaus, P.; Gerber, G. *Nature* **2001**, *414*, 57.
(11) Brixner, T.; Kiefer, B.; Gerber, G. *Chem. Phys.* **2001**, *267*, 241.
(12) Vajda, S.; Bartelt, A.; Kaposta, C.; Leisner, T.; Lupulescu, C.; Minemoto, S.; Rosendo-Francisco, P.; Wöste, L. *Chem. Phys.* **2001**, *267*, 231.
(13) Shi, A.; Woody, A.; Rabitz, H. *J. Chem. Phys* **1988**, *88*, 6870.
(14) Shi, A.; Rabitz, H. *Chem. Phys.* **1989**, *139*, 185.
(15) Zhu, W.; Botina, J.; Rabitz, H. *J. Chem. Phys* **1998**, *108*, 1953.
(16) Zhu, W.; Rabitz, H. *J. Chem. Phys* **1998**, *109*, 385.
(17) Shi, S.; Rabitz, H. *J. Chem. Phys.* **1990**, *92*, 364.
(18) Sola, I.; Santamaria, J.; Tannor, D. *J. Phys. Chem. A* **1998**, *102*, 4301.
(19) Tannor, D.; Rice, S. *J. Chem. Phys.* **1985**, *83*, 5013.
(20) Tannor, D.; Kosloff, R.; Rice, S. *J Chem. Phys* **1986**, *85*, 5805.
(21) Kosloff, R.; Rice, S.; Gaspard, S.; Tersigni, S.; Tannor, D. *Chem. Phys.* **1989**, 201.
(22) Geppert, D.; Hofmann, A.; de Vivie-Riedle, R. *J. Chem. Phys.* **2003**, *119*, 5901.
(23) Manz, J.; Sundermann, K.; de Vivie-Riedle, R. *Chem. Phys. Lett.* **1998**, *290*, 415.
(24) Full, J.; Daniel, C.; González, L. *Phys. Chem. Chem. Phys.* **2003**, *5*, 87.
(25) Daniel, C.; Full, J.; González, L.; Lupulescu, C.; Manz, J.; Merli, A.; Vajda, S.; Wöste, L. *Science* **2003**, *299*, 536.


**10.1021/ja045652s CCC: $30.25** 

***Scheme 1***

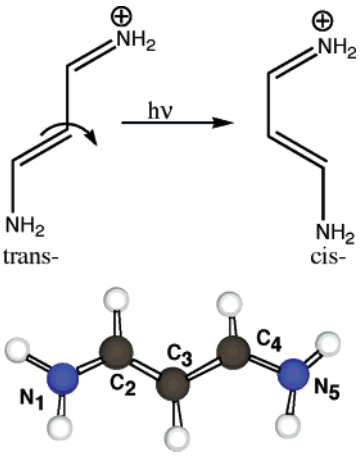


state surface. The subsequent dynamics of the wave packet are complex and are influenced by the location of the conical intersection hyperline or "CI seam", which provides a radiationless decay "funnel" to lower lying electronic states.[26−33] While the lowest energy point of the CI hyperline has often been taken as a model of the photochemical funnel, dynamics computations have recently been used to explore the nature of the CI hyperline away from the minimum and in many cases have shown that other regions of the seam play an important photochemical role.[34−38] In this paper the potential energy surfaces (ground and first excited states) are investigated using molecular dynamics in the full space of the molecular degrees of freedom (semidirect dynamics).[39] The purpose of these computations is to document the nature of the potential energy surface in energetically relevant regions that may lie well away from the minimum energy path. In this way the relevant regions of the potential surface and the nuclear coordinates that dominate the radiationless decay processes are obtained in an unbiased way.

The next step must involve a quantum mechanical treatment of nuclear motion[39−43] and include the laser field explicitly. Such a treatment must obviously be carried out in a low dimension. The results of our semiclassical dynamics will suggest the important nuclear coordinates and also provide a benchmark to compare with the low dimensional quantum mechanical computations. However, we emphasize that the main purpose of our dynamics computations is to show the nature of the potential energy surface and to suggest a strategy whereby coherent control might be obtained.

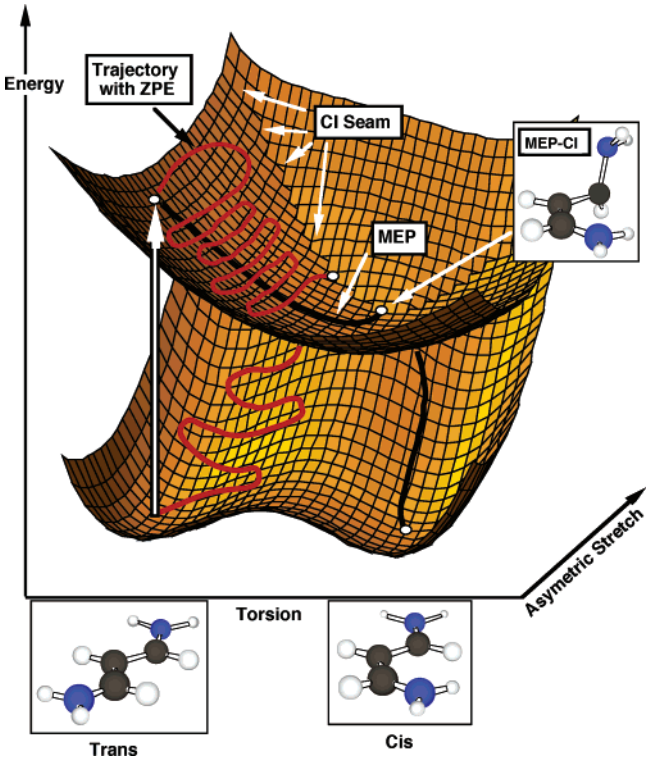


***Figure 1.*** Cartoon representation of the reaction mechanism for ultrafast decay during the trans−cis isomerization of trimethine. Depicted are a typical trajectory (with zero-point energy) and the minimum energy path trajectory. The reaction coordinate is the rotation trans−cis angle, and the branching space coordinates (for simplicity only one of which is included in this diagram) are dominated by symmetric and asymmetric stretch of the terminal C−N bonds.

Our dynamics computations on the trans−cis isomerization of a model cyanine dye, trimethine (Scheme 1), suggest that the potential surface has the form shown in the "cartoon" of Figure 1. (We emphasize that this is only a cartoon of a potential energy surface in the space of two "distinguished" geometrical coordinates; however our dynamics computations are carried out in the full space of (3N-6) geometrical coordinates.) This cartoon shows that the formation of a cis versus trans photochemical product depends on the structure of molecule as it encounters the CI seam. In our model system, we will show that decay to the cis or trans product is controlled by vibrational motion *orthogonal* to the steepest descent reaction path. Accordingly, for a coherent control experiment on a system with this type of surface topology, one could, by controlling the distribution of momentum components in the wave packet, select for decay on the cis or trans regions of the CI seam. Looking at Figure 1, it is clear that decay to the trans product could be achieved by enhancing skeletal stretching (branching space) motions perpendicular to the reaction path. In contrast, an increase in production of the cis product could be achieved by reducing energy in this skeletal motion and enhancing torsional motion. These motions are well separated in energy in the ground-state trans isomer; stretching motions occur 1500−1900 $cm^{-1}$, and torsional motions, 300−700 $cm^{-1}$. In this paper we make an analysis of results obtained from molecular dynamics calculations carried out for the photoinitiated trans−cis isomer-

(26) Atchity, G.; Xantheas, S.; Ruedenberg, K. *J. Chem. Phys.* **1991**, *95*, 1862.
(27) Klessinger, M.; Michl, J. *Excited States and Photochemistry of Organic Molecules*; VCH: New York, 1995.
(28) Yarkony, D. *Rev. Mod. Phys.* **1996**, *68*, 985.
(29) Yarkony, D. *Acc. Chem. Res.* **1998**, *31*, 511.
(30) Yarkony, D. *J. Phys. Chem. A* **2001**, *105*, 6277.
(31) Bernardi, F.; Olivucci, M.; Robb, M. *Chem. Soc. Rev.* **1996**, *25*, 321.
(32) Robb, M.; Garavelli, M.; Olivucci, M.; Bernardi, F. In *Reviews in Computational Chemistry*; Lipkowitz, K., Boyd, D., Eds.; Wiley-VCH: New York, 2000; Vol. 15, p 87.
(33) Olivucci, M.; Migani, A. In *Conical Intersections: Electronic Structure, Dynamics and Spectroscopy*; Domcke, W., Yarkony, D., Köppel, H., Eds.; World Scientific: 2004; Vol. 15.
(34) Migani, A.; Robb, M.; Olivucci, M. *J. Am. Chem. Soc.* **2003**, *125*, 2804.
(35) Müller, H.; Köppel, H.; Cederbaum, L. *New J. Chem.* **1993**, *17*, 7.
(36) Laino, T.; Passerone, D. *Chem. Phys. Lett.* **2004**, *389*, 1.
(37) Garavelli, M.; Celani, P.; Fato, M.; Bearpark, M.; Smith, B.; Olivucci, M.; Robb, M. *J. Phys. Chem. A* **1997**, *101*, 2023.
(38) Ciminelli, C.; Granucci, G.; Persico, M. *Chem.−Eur. J.* **2004**, *10*, 2327.
(39) Worth, G.; Robb, M. *Adv. Chem. Phys.* **2002**, *124*, 355.
(40) Worth, G.; Hunt, P.; Robb, M. *J. Phys. Chem. A* **2003**, *107*, 621.
(41) Domcke, W.; Stock, G. *Adv. Chem. Phys.* **1997**, *100*, 1.
(42) *Faraday Discussions*; Child, M., Robb, M. A., Eds.; Royal Society of Chemistry, 2004; Vol. 127.
(43) Baer, M., Billing, G. *Adv. Chem. Phys.* **2002**; *124*.

*Scheme 2*

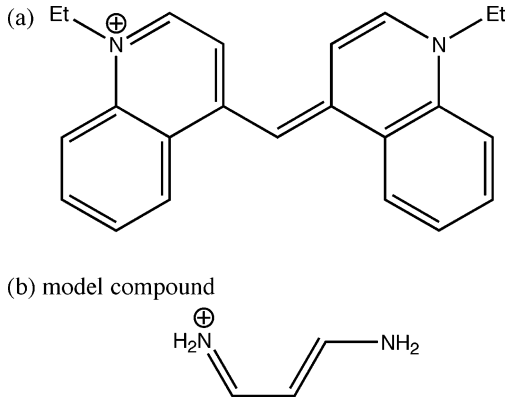


ization of a model cyanine dye. We believe this analysis can provide important insights into the mechanisms controlling fluorescence in the real compound.

The cartoon in Figure 1 is consistent with our previously characterized minimum energy path (MEP) computations.[44] In our previous work, we showed that the $S_1$ MEP from the Franck−Condon (FC) region was dominated by skeletal deformation (single double bond inversion) together with a barrierless rotation about the central bond (trans−cis isomerization). The MEP terminates at a half twisted $S_1$ minimum. Nearby, there is a "tipped" conical intersection.[26] In this work, the detailed nature of the extended conical intersection seam has been extracted from our dynamics simulations as the geometries where the nonadiabatic event or surface hop occurs.

Time-resolved spectroscopic experiments on 1,1′-diethyl-4,4′-cyanine (Scheme 2a) have been carried out by Sundström et al.[45] In the fluorescence up-conversion experiments carried out by Sundström, decay of fluorescence intensity in the Frank−Condon region showed a bimodal distribution composed of an ultrafast and a slower decay component. Sundström suggested that the observation of an ultrafast component for fluorescence decay was consistent with relaxation down the MEP. Further at low energies, the ultrafast component becomes an ultrafast rise time. Sundström suggested that this should be associated with a buildup of population near the minimum of the potential energy surface. Nevertheless, based purely on these observations the possibility of additional decay channels cannot be excluded. Based on additional information derived from our theoretical investigation, we are suggesting a modification to the mechanistic rationalization made by Sundström. (Although, both the original and new mechanisms are consistent with the experimental observations.) In particular, our dynamics results suggest that the slow component observed in the experiments at both high and low energy should be assigned to decay through an extended CI seam that runs roughly parallel (but at a higher energy) to the reaction path.

Sundström's experiments were carried out in several different solutions. The time constants obtained in hexanol were much longer than those obtained in propanol. It was suggested that this was due to solvent drag on the bulky quinoline rings. Our dynamics computations have been carried out on a model system where the quinoline rings are absent, and thus our time scales can be expected to be much shorter.

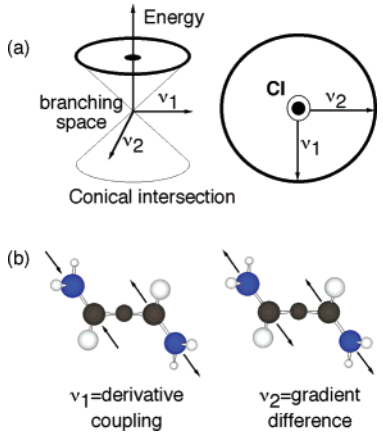


***Figure 2.*** (a) Diagram showing the conical intersection cone; depicted are the axes $\nu_1$ derivative coupling and $\nu_2$ gradient difference. (b) The derivative coupling and gradient difference vectors calculated for the $C_2$ symmetry conical intersection of the model compound.

The cartoon shown in Figure 1 is crucial to understanding the dynamics results. Accordingly we conclude this introduction with a brief discussion of the geometrical coordinates which are labeled "torsion" and "asymmetric stretch" in Figure 1. The reaction coordinate is the trans−cis isomerization about the central double bond. The two vectors, Figure 2a, that lift the degeneracy at a conical intersection span the branching space. For the cyanine model compound these vectors are the symmetric and asymmetric skeletal deformation coordinates ($\nu_1$ $\nu_2$) shown in Figure 2b. Thus the coordinate labeled "branching" space in Figure 1 lies in the space of the two vectors shown in Figure 2b. The conical intersection in Figure 1 appears as a seam (rather than a point) because only one coordinate is taken from the (two-dimensional) branching space and the other is taken from the ($n$−2-dimensional) "intersection" space.

## 2. Theoretical and Computational Details

We have carried out 200 "on-the-fly" trajectory calculations where the nuclear gradient and Hessian are calculated in the full space of all 3N-6 coordinates.[46,47] The gradients are obtained using a complete active space SCF method (CAS-SCF) with a 6-31G* basis set as implemented in the Gaussian suite of programs.[48] The active space used comprises the 5 $\pi$ orbitals and 6 $\pi$ electrons necessary to describe the making or breaking of the 4 $\pi$ bonds.

The CASSCF method[49] has been shown to reproduce potential energy surface topology of photochemical reactions qualitatively, both in general[37,50−52] and for this reaction in particular.[44] In a previous paper,

(44) Sanchez-Galvez, A.; Hunt, P.; Robb, M.; Olivucci, M.; Vreven, T.; Schlegel, H. *J. Am. Chem. Soc.* **2000**, *122*, 2911.
(45) Yartsev, A.; Alvarez, J.; Åberg, U.; Sundström, V. *Chem. Phys. Lett.* **1995**, *243*, 281.
(46) Helgaker, T.; Uggerud, E.; Jensen, H. *Chem. Phys. Lett.* **1990**, *173*, 145.
(47) Chen, W.; Hase, W.; Schlegel, H. *Chem. Phys. Lett.* **1994**, 436.
(48) Frisch, M. J.; Trucks, G. W.; Schlegel, H. B.; Scuseria, G. E.; Robb, M. A.; Cheeseman, J. R.; Zakrzewski, V. G.; Montgomery, J. A., Jr.; Stratmann, R. E.; Burant, J. C.; Dapprich, S.; Millam, J. M.; Daniels, A. D.; Kudin, K. N.; Strain, M. C.; Farkas, O.; Tomasi, J.; Barone, V.; Cossi, M.; Cammi, R.; Mennucci, B.; Pomelli, C.; Adamo, C.; Clifford, S.; Ochterski, J.; Petersson, G. A.; Ayala, P. Y.; Cui, Q.; Morokuma, K.; Malick, D. K.; Rabuck, A. D.; Raghavachari, K.; Foresman, J. B.; Ortiz, J. V.; Baboul, A. G.; Cioslowski, J.; Stefanov, B. B.; Liu, G.; Liashenko, A.; Piskorz, P.; Komaromi, I.; Gomperts, R.; Martin, R. L.; Fox, D. J.; Keith, T.; Al-Laham, M. A.; Peng, C. Y.; Nanayakkara, A.; Gonzalez, C.; Challacombe, M.; Gill, P. M. W.; Johnson, B.; Chen, W.; Wong, M. W.; Andres, J. L.; Gonzalez, C.; Head-Gordon, M.; Replogle, E. S.; Pople, J. A. *Gaussian 99*, Development Version (revision C.01) ed.; Gaussian, Inc.: Pittsburgh, PA, 1999.
(49) Yamamoto, N.; Vreven, T.; Robb, M.; Frisch, M.; Schlegel, H. *Chem. Phys. Lett.* **1996**, *250*, 373.
(50) Weingard, O.; Migani, A.; Olivucci, M.; Robb, M.; Buss, V.; Hunt, P. *Phys. Chem. A* **2004**, *108*, 4685.
(51) Boggio-Pasqua, M.; Bearpark, M.; Hunt, P.; Robb, M. *J. Am. Chem. Soc.* **2002**, *124*, 1456.
(52) Paterson, M.; Hunt, P.; Robb, M. *J. Phys. Chem. A* **2002**, *106*, 10494.

we have compared the CASSCF trans−cis isomerization of trimethine PES (at critical points) against methods that include dynamical correlation. Discrepancies were found at the quantitative level; however, the CASSCF method reproduced a qualitatively correct PES.[44] Moreover, our trajectories were run with a significant amount of excess energy and thus explore the potential energy surface well above the minimum energy path. Under these circumstances the effects we see are mainly determined by the surface topology. The errors in energetics will mainly affect time scales.

In the dynamics computations, the initial conditions were determined by random sampling[53,54] of the ground state zero-point (ZP) vibrations which generated a set of (deformed) coordinates and (nonzero) velocities. We have previously shown that such sampling can accurately model the approach to a conical intersection.[40] It has been shown that a swarm of classical trajectories can (in the short time limit) reproduce the results of computations where the nuclear motion is treated quantum mechanically.[20]

Our direct dynamics algorithm includes surface hopping.[55] Trajectories were propagated on an adiabatic surface, until a region of strong nonadiabatic coupling was encountered. At this point state-averaged CASSCF was used to ensure both surfaces were treated at the same level. A time dependent electronic wave function (which is a mixture of the CASSCF adiabatic states) was propagated (in concert with the nuclear dynamics) as a solution to the time-dependent Schrödinger equation. The surface hopping probabilities were determined from the weights of the adiabatic states in this wave function. Trajectories were halted shortly after a hop. In the dynamics calculations each point on each trajectory (near the CI seam) requires the solution of SA-CP-MCSCF[56−59] equations with 30 degrees of freedom.

Computation of a fluorescence spectrum[60,61] for the model trimethine compound is not feasible because of the extremely fast deactivation time. In our computations the aromatic rings and solvent effects are missing. Time scales are significantly affected and are an order of magnitude faster than those in the target system.

## 3. Results and Discussion

**Analysis of a Representative Trajectory.** We begin our discussion by looking at a representative trajectory in some detail. Figure 3a shows the energy of $S_0$ and $S_1$ (minus a constant, $E_{S_1min}$) versus time for a typical trajectory, and their difference gives the time dependent $S_1/S_0$ energy gap. The decrease in size of the energy gap over time is *not* due to a decrease in the energy of the excited state but is dominated by an increase in the energy of the ground state. The initially sampled velocities and geometries for this trajectory are shown in Figure 4a and 4b, respectively. The computed trajectory has two distinct phases. In the first part of the trajectory (0−45 fs), the $S_0/S_1$ energy gap decreases rapidly as the molecule moves away from the FC point toward the CI seam, and a quasi trans-like geometry, Figure 4c. A comparison of Figure 3b (bond lengths) and 3c (torsion angle) indicates that this initial motion is dominated by skeletal deformation, with local stretching of the $C_3-C_4$ bond (atomic labels are given in Scheme 1). However, decay does not occur on the first close encounter with the CI seam because the energy gap is still relatively large, 6.27 kcal mol$^{-1}$ (26.25 kJ mol$^{-1}$), and the system continues to evolve on the excited state surface $S_1$. (A graph showing the evolution of the electronic population over time is included in the Supporting Information.) In the second phase, after 60 fs, twisting begins, Figure 4c, followed by decay at 89 fs through the CI seam (close to the minimum on $S_1$) at a cis-like geometry, Figure 4d. Once a molecule has decayed it evolves on the ground state; the probability of a "jump up" is close to but not exactly zero. An advantage of using the CASSCF method is that we can monitor both the ground and excited states at the same time, irrespective of which state is driving the dynamics. Notice that skeletal relaxation is fast and that by 60 fs the $C_3-C_4$ bond length is already 1.7 Å. This allows the two ends of the cyanine molecule almost free rotation relative to each other. A distinguishing feature of most trajectories is a smooth and steady change along this torsional "reaction coordinate". The lower

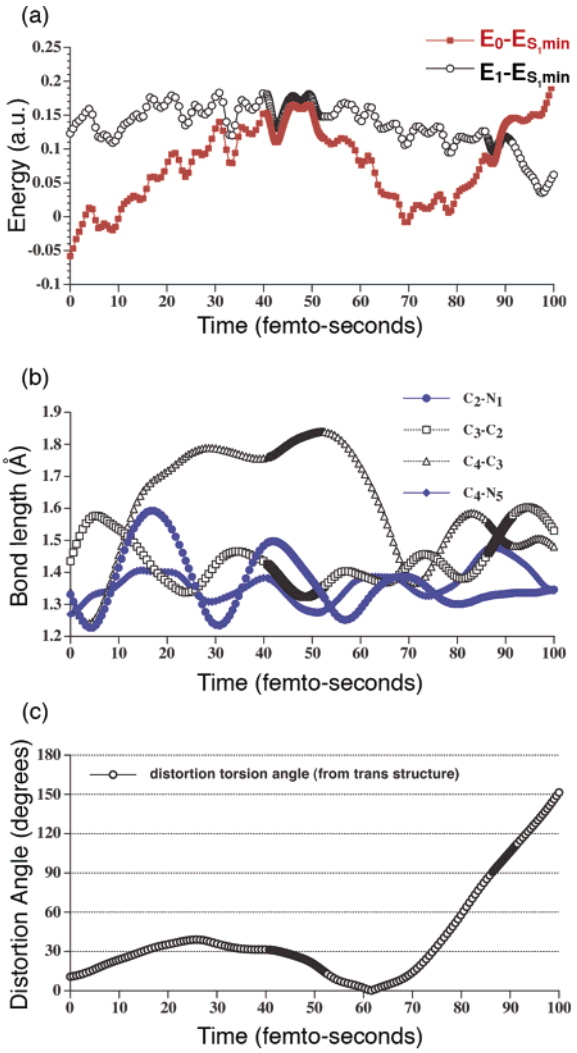


***Figure 3.*** (a) Energy profile for a typical trajectory, the energies shown are reported relative to the (time independent) energy of the local $S_1$ minimum. (b) Bond length oscillations over time for a typical trajectory. Solid lines and points (circles and diamonds) show terminal C−N bonds, dashed lines and open points (squares and triangles) show internal C−C bonds. When the trajectory enters a region of nonadiabatic coupling, the time step is reduced giving rise to an increase in the density of points. (c) Level of distortion from the trans structure as measured by the angle theta, $\tau = \text{abs}[\theta_1 + \theta_2 - 360°]$ where $\theta_1 = \tau(N_1-C_2-C_3-C_4)$ and $\theta_2 = \tau(N_5-C_4-C_3-C_2)$ (see Figure 4) where the range of $\theta_1$ and $\theta_2$ is 0−360° and thus $\tau = 0°$ in *trans*-trimethine and $\tau = 180°$ in *cis*-trimethine.

(53) Sloane, C.; Hase, W. *J. Chem. Phys.* **1977**, *66*, 1523.
(54) Chapman, S.; Bunker, P. *J. Chem. Phys.* **1975**, *62*, 2890.
(55) Tully, J.; Preston, R. *J. Chem. Phys.* **1971**, *55*, 652.
(56) Lengsfield, B. *J. Chem. Phys.* **1980**, *73*, 382.
(57) Diffenderfer, R.; Yarkony, D. *J. Chem. Phys.* **1982**, *77*, 5573.
(58) Werner, H.; Meyer, W. *J. Chem. Phys.* **1981**, *74*, 5794.
(59) Page, M.; Saxe, P.; Adams, G.; Lengsfield, B. *J. Chem. Phys.* **1984**, *81*, 434.
(60) Walker, R.; de Souza, M.; Mercer, I.; Gould, I.; Klug, D. *J. Phys. Chem. B* **2002**, *106*, 11658.
(61) Mercer, I.; Gould, I.; Klug, D. *J. Phys. Chem. B* **1999**, *103*, 7720.

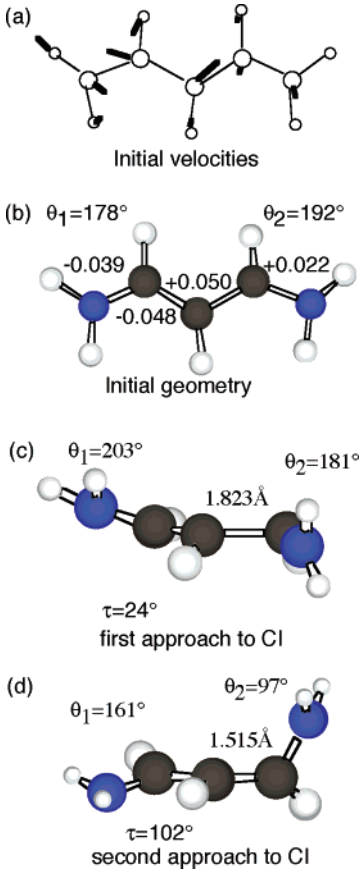


***Figure 4.*** Initial velocity (a) and displacement (b) for the typical trajectory analyzed in Figure 3, and the geometry of the cyanine molecule in the region of the CI on (c) the first approach and (d) the second approach (at which decay occurs). In model b the numbers above and below selected bonds in the N−C−C−C−N backbone indicate the extent of distortion from the ground state geometry. In models b−d the terminal torsion angles $\theta_1 = \tau(N_1{-}C_2{-}C_3{-}C_4)$ and $\theta_1 = \tau(N_5{-}C_4{-}C_3{-}C_2)$ are given. Theta is the deviation from a trans conformation, $\tau = \text{abs}[\theta_1 + \theta_2 - 360°]$ where the range of $\theta_1$ and $\theta_2$ is 0−360° and thus $\tau = 0°$ in *trans*-trimethine and $\tau = 180°$ in *cis*-trimethine. In models c and d the bond length of the highly stretched $C_3{-}C_4$ bond is given. Numerical data are available in the Supporting Information.

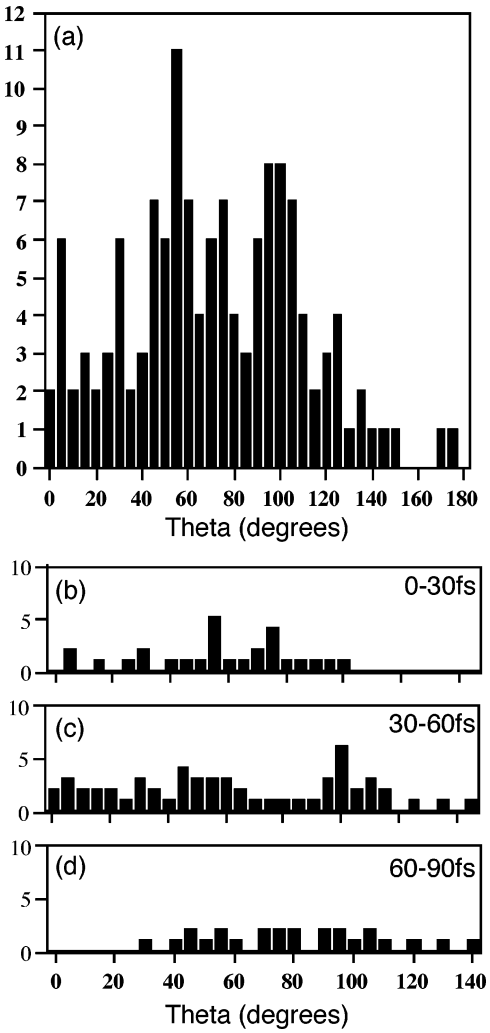


***Figure 5.*** Distribution of the angle theta when molecules pass through the CI seam. Theta is the deviation from a trans conformation, $\tau = \text{abs}[\tau_1 + \tau_2 - 360°]$ where $\theta_1 = \tau(N_1{-}C_2{-}C_3{-}C_4)$ and $\theta_2 = \tau(N_5{-}C_4{-}C_3{-}C_2)$ where the range of $\theta_1$ and $\theta_2$ is 0−360° and thus $\tau = 0°$ in *trans*-trimethine and $\tau = 180°$ in *cis*-trimethine. The insets b−d show the angles theta for molecules passing through the CI seam over the time intervals (a) 0−30 fs, (b) 30−60 fs, and (d) 60−90 fs.

frequency rotational motion is thus superimposed on higher frequency degeneracy breaking (bond stretching) vibrations. Cis−trans torsional motion leads down the MEP, while bond stretching motions (orthogonal to the torsional vibration) lead toward the CI seam. Thus the locus of radtionless decay (crucially) depends on the relative kinetic energy in these skeletal and torsional coordinates. The oscillatory features in Figure 3a and b differ because Figure 3b represents a *single* vibrational mode, while the rapid oscillations in the fine structure of Figure 3a reflect a rapid exchange of kinetic and potential energy within *all* the vibrational modes.

**Global Analysis of Dynamics Data.** We now turn to a global analysis of our trajectory results. Of course, given the small number of trajectories, we cannot claim statistical validity. Nevertheless, we believe that the general trend is already completely obvious and thus some general conclusions can be drawn.

Figure 5a shows the twist angle (reaction coordinate) at the nonadiabatic hop to $S_0$ for all our trajectories. Figure 5b−d show the angular distribution over various time intervals. These data need to be examined in conjunction with Figure 6 where we have shown the excited state population corresponding to a given ground to excited state energy gap. In interpreting Figure 6 we associate the largest energy gap, Figure 6a, with the Franck−Condon region, and the smallest energy gap, Figure 6d, with the region adjacent to the CI seam. Remember that Figure 3 contains data for a single trajectory, while Figures 5 and 6 represent data for *all* 200 trajectories.

We begin with a discussion of the data showing the twist angle irrespective of time, Figure 5a. It is clear that the hop geometries span a full range of twist angles, and thus, the CI seam is energetically accessible at all twist angles. This verifies the topological features depicted in the cartoon of Figure 1 and demonstrates that the CI seam runs roughly parallel to the reaction path.

The population shown in Figure 6a corresponds, at least approximately, to the population in the Franck−Condon region. There are clearly two temporal distributions, a fast and slow decay, in agreement with the experiments of Sundström et al.

Now let us consider the "shape" of the wave packet in the region of the conical intersection seam (that is, the population versus distribution in twist angle plus branching space coordi-

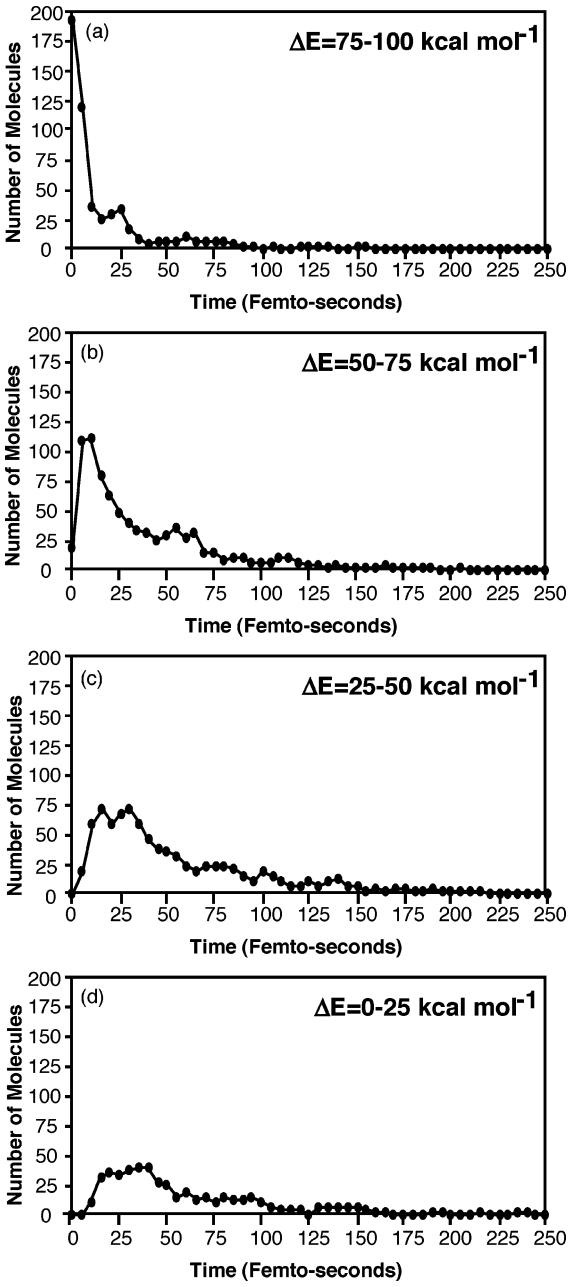


***Figure 6.*** Number of molecules on $S_1$ with an energy gap $\Delta E = E_1 - E_0$ among (a) 75−100 kcal/mol, (b) 50−75 kcal/mol, (c) 25−50 kcal/mol, and 0−25 kcal/mol plotted against the time (in 5 fs intervals). Note that molecules can pass through an energy domain and then re-enter it at a later time and that decay through an CI seam results in a gradual population loss.

nate). This information is obtained by comparing the data in Figure 5 (hop geometry) with the data in Figure 6d ($S_1$ population with a small energy gap). First, from Figure 5, it can be seen that, by the time the wave packet reaches the CI seam, almost all twist angles are populated. Thus upon leaving the Franck−Condon region, the wave packet has spread very rapidly to cover all twist angles, within the first 30 fs as shown in Figure 5b. The wave packet then evolves toward the CI seam more slowly. This can be seen by comparing the initial decay shown in Figure 6a, corresponding to rapid movement out of the FC region (and along the reaction coordinate), with the slower decay features of Figures 6c and 6d. The rise time shown in Figure 6c and 6d correlates with the population decay in Figure 6a and corresponds to the increasing population in the region of the CI seam. Thus the fast process is associated with trans−cis twisting, and the slower process can be associated with spread of the wave packet toward CI seam. Thus, the wave packet rapidly spreads down the reaction coordinate (minimum energy path) and then expands perpendicular to this up into the CI seam.

How does the previously discussed sample trajectory (Figure 3) contribute to this global picture (Figures 5 and 6)? We chose this particular trajectory because it contains, on a time scale slightly slower than the average trajectory, many important features. The sample trajectory approaches the CI more slowly than the average trajectory; most take <60 fs to reach the CI and contribute to Figure 5b and c. The sample trajectory, unlike the bulk of trajectories, does not hop on the first approach to the CI but continues to evolve on the excited state, hopping relatively late at 89 fs, and thus contributes to Figure 5d. Accordingly, on average, the hop time is much shorter and the torsion is much faster than depicted in the sample trajectory.

We briefly summarize the salient points of the previous discussion. Our dynamics results are consistent with the cartoon shown in Figure 1 and demonstrate the existence of an extended conical intersection seam. Our dynamics show that by the time the wave packet reaches this seam essentially all torsional angles are populated. The general form of the excited-state populations with a large energy gap (Franck−Condon region) and small energy gap (vicinity of the CI seam) shown in Figure 6 are consistent with the experimental results obtained by Sundström et al. However, the dynamics calculations have shown that the mechanistic process at a small energy gap is consistent with a wave packet containing a wide distribution of twist angles, rather than evolution to the fully twisted geometry (ca. 107°) and then subsequent decay.

Finally, we should comment that the dynamics observed here are in marked contrast with the *Z*→*E* photoisomerization of the *Z*-pentadieniminium cation, a minimal model for the biologically relevant chromophore retinal.[13] While the CI seam in the *Z*-pentadieniminium cation system extended to regions of zero twist, the dynamics showed (in contrast to the current case) that the seam is only accessed near the minimum CI point (i.e., at twist angles 70°−92°) and thus is not sampled for small twist angles. This selectivity is a result of the shape of the $S_1$ surface, and the position of the CI seam relative to the MEP.

## 4. Conclusions

The dynamics results presented in this paper suggest a potential energy surface of the form shown in Figure 1 for the model cyanine dye, trimethine. The dynamics results reported in Figure 6 (showing the time decay of the excited state populations) are in qualitative agreement with experiment.[5] This lends some consistency to the theoretical observation that the nonadiabatic transition (or surface hop) takes place over a complete range of twist angles (from trans to cis) and not just at the minimum energy point on the conical intersection seam.

In the interpretation of their experiments Sundström et al. assumed the simple model of "sand flowing through a funnel". They assumed that radiationless deactivation occurred only after the system had evolved to the excited-state minimum on the potential surface. In contrast, our dynamics results suggest that radiationless decay occurs along an extended conical intersection seam.

These results suggest a molecular mechanism for coherent control that might be used to provide a new paradigm for coherent control experiments. In the current dynamics computations, initial conditions were determined by the zero-point energy distribution of the ground state. In a coherent control experiment one could attempt to control and change the momentum components of the wave packet and hence select for decay at the cis or trans regions of the CI seam.

The theoretical design of a coherent control sequence must ultimately involve running theoretical dynamics on a computed potential energy surface where the laser field is explicitly included. The model for this can be seen, for example, in the theoretical work of de Vivie-Riedle[22,23] or Gonzâlez,[24] where both optimal control methods and wave packet dynamics have been used. The point that we have established in this paper is that, because of the extended low-energy conical intersection seam, this type of system might be a useful prototype for coherent control experiments. Our results suggest a wave packet with significant components near the C−N stretching frequencies (1900 $cm^{-1}$) or momentum components perpendicular to the reaction path might force the wave packet through high energy points of the CI seam resulting in preferential formation of the trans-isomer, while a wave packet with very little contribution from the high energy region of the spectrum should propagate the wave packet along the torsional reaction path (300−700 $cm^{-1}$), resulting in preferential formation of the cis-isomer. Designing an actual laser pulse sequence needs both optimal control methods and wave packet dynamics. Experimentally, this would need to be combined with a learning algorithm and feedback loop strategy.

**Acknowledgment.** All calculations were carried out on an IBM-SP2 jointly funded by IBM-UK and HEFCE (UK). P.H. is grateful to the EPSRC for her postdoctoral grant and the Royal Society for her University Research Fellowship.

**Supporting Information Available:** The following Supporting Information is available: the initial Cartesian coordinates and mass weighted velocities for the representative trajectory (au); Cartesian coordinates in pdb file format (and structure diagram) of the initial Cartesian coordinates, geometry at first approach to the conical intersection, and hop geometry; tabulated data used to generate Figure 3 for the duration of the representative trajectory; a graph showing the evolution of the electronic population over time. This material is available free of charge via the Internet at http://pubs.acs.org.

JA045652S